A&A 411, L127–L129 (2003)
DOI: 10.1051/0004-6361:20031204

Astronomy & Astrophysics

Maximum Entropy imaging with INTEGRAL/SPI data

A. W. Strong⋆

Max-Planck-Institut für extraterrestrische Physik, Postfach 1312, 85741 Garching, Germany

Received 14 July 2003 / Accepted 5 August 2003

Abstract. The application of the Maximum Entropy method for sky imaging with the SPI instrument on INTEGRAL is described. While intended primarily for extended emission, point sources are also mapped by this method. The technique is implemented as the program *spiskymax* in the data analysis distribution provided by the INTEGRAL Science Data Centre. We briefly introduce the method, describe the particular requirements for the application to SPI, and show some example images using flight data from the early mission.

Key words. data analysis – gamma rays – coded masks – INTEGRAL

1. Introduction

The coded-mask imaging γ-ray spectrometer SPI (Vedrenne et al. 2003; Attié et al. 2003; Roques et al. 2003) on the INTEGRAL Observatory (Winkler et al. 2003) is designed to study point sources and map diffuse extended emission with an angular accuracy of about 2° over its energy range of ~20–8000 keV. The purpose of the maximum entropy software package described here is to represent the measurements in terms of pixelized models of the sky, including estimates of the uncertainty. This tool is oriented towards large-scale surveys (e.g. GCDE), which combine a large set of individual pointings of the spacecraft. It concentrates on spatial as opposed to spectral information, although (using images in multiple channels) it could be a useful method to generate spectra of diffuse emission. The principal use of the method is generating maps of γ-ray emission in lines and continuum. Examples are the 1809 keV ^{26}Al line and diffuse continuum γ-rays. The analysis of SPI data with this tool is complementary to methods specifically designed for point sources such as *spiros* (Skinner et al. 2003), other imaging methods such as Richardson-Lucy (Knödlseder et al. 2003) and spatial model-fitting techniques (Strong et al. 2003). A critical comparison of the maximum entropy method with other methods such as MREM is given by Knödlseder et al. (1999).

The method has been applied extensively to CGRO/COMPTEL data for both diffuse lines (Plüschke et al. 2000) and continuum (Strong et al. 1999a) and therefore the idea to use it for INTEGRAL data appeared natural.

The algorithm performs fitting of raw data (binned counts for many observations) to a pixelated sky model using the full instrument response information. In addition to sky imaging, the method can be used to obtain profiles (intensities integrated over one dimension) and source fluxes, in both cases with error estimates. The package is referred to as *spiskymax*.

⋆ e-mail: aws@mpe.mpg.de

This short paper provides only a general introduction to *spiskymax* with first illustrative examples of its use on flight data; a detailed evaluation of the performance in terms of source location accuracy, flux determination and possible appearance of artefacts, will take much more analysis and is beyond the scope of this paper.

2. The MaxEnt algorithm

2.1. Principles

The Maximum Entropy method (MaxEnt) is a general technique for deconvolution of data, which has been developed over the past 25 years with special emphasis on applications in spectrosopy and imaging. The implementation in *spiskymax* is based on the MEMSYS5 package which uses advanced numerical techniques to perform the computations, which are challenging on account of the large dimensionality of the problem. The standard papers on the method are Skilling (1989) and Gull (1989). A good exposition of the principles can be found in Sivia (1997) as well as the literature associated with the MEMSYS5 package itself. MaxEnt is described in detail in the MEMSYS5 User's Manual[1], and the reader is referred to this for a full exposition. Extensive details of the *spiskymax* algorithm, the use of the package and references to related literature are given in the User Manual, available from the INTEGRAL Science Data Centre[2].

The original "maximum entropy method" as applied to imaging was based on the idea of smoothness, the principle being to obtain the "flattest image consistent with the data", where "flatness" is measured by the entropy defined as the sum over pixels $S = -\sum_i p_i \ln p_i$, where p_i is the fraction (proportion) of the image flux in pixel i. These arguments are

[1] Available from http://www.maxent.co.uk
[2] http://isdc.unige.ch

given in detail in the literature, but the basic principle is to generate a "conservative" solution which contains "only structure for which there is evidence in the data". Note that in this form the entropy does not incorporate smoothness in the sense of pixel-to-pixel correlations.

Although the original applications were very effective there were conceptual problems. In particular, there was no justifiable stopping criterion, and error estimation was not possible. The further conceptual developments leading to MEMSYS5 came from formulating the method as a particular application of Bayesian statistics, with entropy providing the basis for the prior probabilities. This "Quantified Maximum Entropy" or "Classic Maximum Entropy" is based on the concept of the posterior probability distribution in the full N-dimensional space of image pixels, and this allows explicit computation of uncertainties and a well-defined criterion for the "best" image.

2.2. MaxEnt formulae

I give here a brief summary of the main formulae involved, omitting technicalities. The posterior probability of the image I given the data D is $P(I|D) \propto e^{L+\alpha S}$ where $L = \ln P(D|I)$ is the log-likelihood function and $S = \sum_i (I_i - m_i - I_i \ln \frac{I_i}{m_i})$ is the entropy in the form appropriate to "positive additive distributions". It can be shown (Skilling 1989) that this form of S is the only one possessing the necessary invariance properties such as coordinate invariance. Here m_i is the default value to which a pixel will be assigned in the absence of constraints from the data (S is maximum at $I = m$). The parameter α, which determines the balance between the influence of the prior and the data on the result, is in principle unknown; however in Classical MaxEnt α can itself be treated by Bayesian methods and ideally "marginalized" out; in practice a best value is determined by maximizing the probability of the data $P(D)$. It can be shown (Gull 1989) that the best value corresponds to equating the amount of structure in the image with the "number of good measurements" in the data. In cases where this estimate of α is not adequate, an option to treat it as a user-defined parameter can be invoked. The parameter m is generally taken to define a "flat" image, with a value approximately equal to the mean expected intensity; the exact value is not critical.

The MEMSYS5 package performs an iterative search to obtain $P(I|D)$. This can then be used to compute "error bars" on any linear combination of the pixels, allowing profiles across the image or fluxes of point sources with their associated uncertainties to be generated.

3. The MaxEnt method applied to SPI data

The response of the instrument, as a function of direction, energy and detector is based on the extensive simulations and parameterization by the Goddard group (Sturner et al. 2003). In the data and response both single detector and multiple detector events are handled. Poisson statistics are used throughout, since SPI counts are in general small numbers.

The application to SPI is complicated by the necessity to handle the background in a flexible way. The background is modelled using either a set of "OFF" observations, or using tracers of the cosmic-ray activity in the detectors (e.g. "saturating events"). The time-dependence of the background can also be derived using model-fitting (*spidiffit* program). The background parameters are determined simultaneously with the image as part of the iterative procedure. Options to fit the background per detector (externally determined time dependence) or as a function of time (externally determined detector ratios) are available.

One image is produced per energy range of the input data, and parameters like sky area, binsize, background method etc. can be set by the user. Source positions for analysis are specified via a source catalogue, and the parameters of the required profiles (longitude/latitude, binning) can be specified.

The source location accuracy of *spiskymax* on point-sources depends on the available statistics, but for a typical source of the flux of 1E1740-2942 it is ~0.5°. Flux determinations for sources at known positions are found to agree within errors to those from other methods such as *spiros*. *spiskymax* has the advantage of explicitly including the diffuse background from the Galactic plane, especially intense at low energies (Strong et al. 2003).

4. Illustrative applications

Pre-flight simulations of *spiskymax* imaging of diffuse continuum emission can be found in Strong et al. (1999b). An example of the performance of *spiskymax* on pre-launch calibration data is given in Attié et al. (2003), showing the separation of sources at 2° and 1° separation. Extensive evaluations of *spiskymax* on data taken with a SPI laboratory test setup are given in Wunderer et al. (2003). While providing an essential validation of the method, these pre-launch calibrations have a much higher signal-to-noise ratio than in flight, and hence illustrates only the ideal performance. In this paper we show examples from flight data.

4.1. Cygnus region

During the Performance Validation phase of INTEGRAL the Cygnus region was observed and this gave the first chance to test the imaging under flight conditions. A detailed study of this region using SPI data is given by Bouchet et al. (2003). Figure 1 shows a *spiskymax* image in the 200–400 keV range, using single event data for Cygnus observations from revolutions 11 to 25, and a background template from revolutions 12 and 13 (which were pointed towards high latitudes and specifically chosen as empty fields containing no strong sources for the Performance Validation). The background time-dependence was free in this example, being determined by *spiskymax* along with the image. The field is dominated by the source Cyg X-1 which appears at the correct position to within the 0.5° binning. The scale is logarithmic to show up the low levels: the faint artefacts are at a level of only 2% of the source peak. However this data does not provide a particularly challenging test for *spiskymax* , due to the limited number of objects in the field at γ-ray energies.

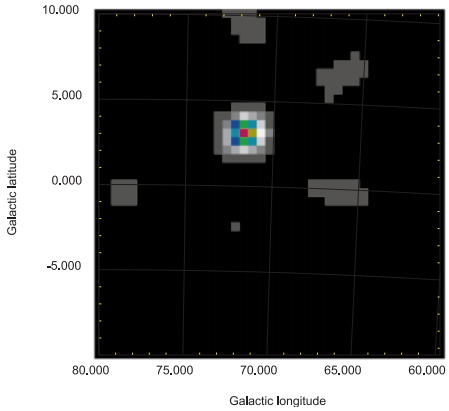

Fig. 1. *spiskymax* image of the Cygnus region in energy range 200–400 keV, using Performance Validation Phase SPI data.

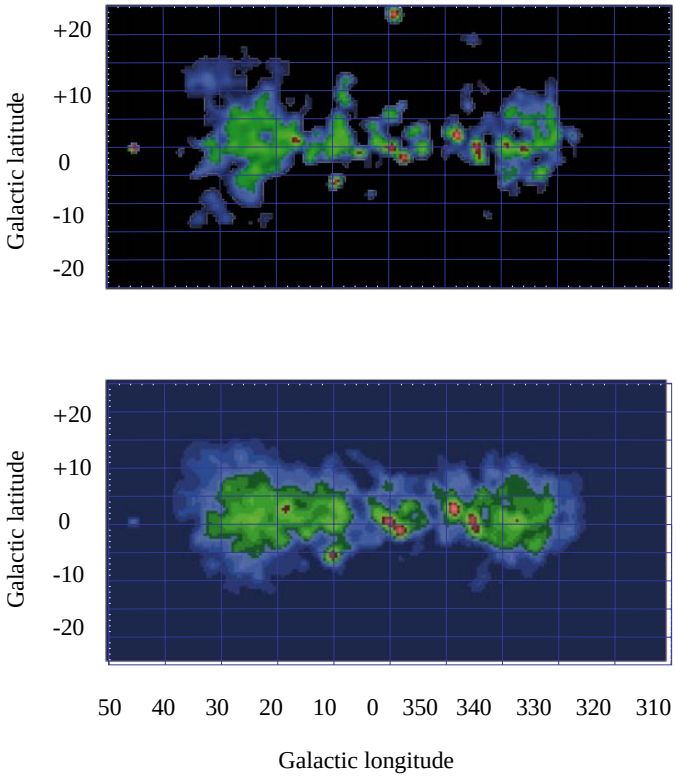

Fig. 2. *spiskymax* images of the inner Galaxy in energy ranges 18–40 keV (upper) and 40–100 keV (lower), using the first cycle of GCDE SPI data. Sources visible include 4U1700-377 (l = 347.8, b = +2.2), H1741-322 (l = 357.1, b = −1.6), 1E1740.7-2942 (l = 359.1, b = −0.1), Sco X-1 (l = 359.1, b = +23.8), GS1826-238 (l = 8.9, b = −5.3), GRS1915+105 (l = 45.4, b = −0.2).

4.2. Inner Galaxy

The INTEGRAL Core Program includes the Galactic Centre Deep Exposure (GCDE), designed to map the inner Galaxy ($330° < l < 30°, -20° < b < 20°$). The pointings used, from the first complete GCDE cycle and parts of the Galactic Plane Scans, are shown in the paper on the diffuse emission (Strong et al. 2003). The same OFF observations as for the previous example were used. The background detector ratios were free in this example, and the time variation was determined by spatial model fitting to a diffuse model plus sources using the *spiditfit* program (Strong et al. 2003). Skymaps using data in the 18–40 keV and 40–100 keV energy ranges are shown in Fig. 2, with some of the strongest sources identified. The sources listed are all at the correct positions to within the 0.5° pixelization of the image. Diffuse emission from the Galactic plane, which is an intense source in this energy range, is also probably visible in these images, although this remains to be explicitly demonstrated. The inner Galaxy field provides a good test of the performance of *spiskymax* for multiple sources, some at small angular separations, in the presence of diffuse emission. The performance on two close sources, 1E1740-2942 and H1741-322, 2.5° apart, which are clearly separated, is demonstrated by these images.

5. Conclusions

spiskymax has been shown to operate successfully on SPI flight data, and has heen used to generate images of the sources in the inner Galaxy using the first survey data. A demonstration of its application to diffuse line and continuum emission will be the next goal. The method will continue to be developed on the basis of the experience gained; in particular the background treatment, which is based mostly on information obtained since the launch of INTEGRAL, will be pursued.

Acknowledgements. The SPI project has been completed under the responsibility and leadership of CNES. We are grateful to ASI, CEA, CNES, DLR, ESA, INTA, NASA and OSTC for their support.

References

Attié, D., Cordier, B., Gros, M., et al. 2003, A&A, 411, L71
Bouchet, L., Jourdain, E., Roques, J. P., et al. 2003, A&A, 411, L377
Gull, S. F. 1989, in Maximum Entropy and Bayesian Methods, ed. J. Skilling (Dordrecht: Kluwer), ISBN-0-7923-0224-9, 53
Knödlseder, J., Dixon, D., Bennett, K., et al. 1999, A&A, 345, 813
Knödlseder, J., Lonjou, V., Jean, P., et al. 2003, A&A, 411, L457
Plüschke, S., Diehl, R., Schönfelder, V., et al. 2000, AIP Conf. Proc. 510, ed. M. L. McConnell, & J. M. Ryan, 35
Roques, J.-P., Schanne, S., von Kienlin, A., et al. 2003, A&A, 411, L91
Sivia, D. S. 1997, Data Analysis: A Bayesian Tutorial (Oxford University Press), ISBN 0-19-851889-7
Skilling, J. 1989, in Maximum Entropy and Bayesian Methods, ed. J. Skilling (Dordrecht: Kluwer), ISBN-0-7923-0224-9, 45
Skinner, G. K., & Connell, P. H. 2003, A&A, 411, L123
Strong, A. W., Bloemen, H., Diehl, R., Hermsen, W., & Schönfelder, V. 1999a, Astrophys. Lett. Comm., 39, 677
Strong, A. W., Diehl, R., Connell, P., & Skinner, G. K. 1999b, Astrophys. Lett. Comm., 39, 689
Strong, A. W., Bouchet, L., Diehl, R., et al. 2003, A&A, 411, L447
Sturner, S. J., Shrader, C. R., Weidenspointner, G., et al. 2003, A&A, 411, L81
Vedrenne, G., Roques, J.-P., Schönfelder, V., et al. 2003, A&A, 411, L63
Winkler, C., Courvoisier, T. J.-L., Di Cocco, G., et al. 2003, A&A, 411, L1
Wunderer, C. B., Connell, P., Hammer, J. W., Schönfelder, V., & Strong, A. W. 2003, A&A, 411, L101